Available online at www.sciencedirect.com

ScienceDirect

IFAC Papers Online CONFERENCE PAPER ARCHIVE

IFAC-PapersOnLine 49-26 (2016) 044–049

# Parameter estimation for leukocyte dynamics after chemotherapy ⋆

**Kristine Rinke** * **Felix Jost** * **Rolf Findeisen** **
**Thomas Fischer** *** **Rainer Bartsch** *** **Enrico Schalk** ***
**Sebastian Sager** *

* *Institute of Mathematical Optimization, Otto-von-Guericke University, Magdeburg, 39106 Germany (OVGU)*
*(e-mail corresponding author: kristine.rinke@ovgu.de)*
** *Institute for Automation Engineering, OVGU*
*** *Department of Hematology and Oncology, OVGU*

**Abstract:** Leukopenia is one of the most harmful side effects during chemotherapy treatment, since leukocytes (L) are crucial in protecting patients against bacteria and fungi. A personalized mathematical model of dynamics of L would allow a glimpse into the future and the initiation of tailored countermeasures.
We propose such a mathematical model and calibrate it based on a parameter estimation with real world data. For our study we used data of L during and after consolidation chemotherapy treatment (cytarabine) of six patients contracting acute myeloid leukemia.
We compare two different ways to treat the unknown initial values of the system of ordinary differential equations, discuss patient-specificity of parameter values, and different scalings of the least squares formulation. These three comparisons are necessary considerations for all modeling approaches to biomedicine, and have thus a methodological scope beyond the specific case of leukopenia.
In summary, we show that our approach is able to simulate L dynamics in response to chemotherapy treatment and allows to take patient-specific characteristics into account.



*Keywords:* Leukopenia, acute myeloid leukemia, parameter estimation, weighted least-squares method, initial value analysis

## 1. INTRODUCTION

Leukocytes (L) are white blood cells, circulating the blood stream as a part of the immune system, and therefore crucial in protecting humans against bacteria and fungi. Their standard range varies for adults between 4 and 10 thousands cells per microliter. Acute myeloid leukemia (AML) is a common type of leukemia in adults. It is originating in the bone marrow and associated with hematopoiesis, i.e., the process where mature blood cells (MC) differentiate from hematopoietic stem cells (HSC). These HSCs have the capability to proliferate generating either HSCs or precursor cells (PC). There are two lineages of PCs - the myeloid and the lymphoid line - both differentiate through several stages into diverse MCs which are released into the bloodstream as L. AML is characterized by degeneration of cells in early stage within the myeloid line resulting in a rapid increase of so called myeloid blasts, i.e., non-differentiating cells that interfere with the hematopoiesis. Without any therapy, AML is lethal within a few months. Therefore, the initiation of a therapy is usually realized immediately.

The chemotherapy treatment schedule is usually divided into two phases, induction and consolidation, consisting of repeated administrations of chemotherapy infusions. The first usually involves about one or two cycles of induction therapy with complete remission on target. During the last decades, plenty of studies dealt with improving the outcomes of induction, but none of them was able to identify suitable alternatives to the current practice (cf. Eigendorff and Hochhaus (2015)). Therefore, we focus on consolidation therapy, the second period of the treatment schedule.

To maintain complete remission of the induction, it is followed by consolidation with two to four cycles of cytarabine (AraC, $\geq 1000\ mg/m^2$). AraC acts in a two-step process: Firstly it is transformed to AraCTP and, secondly, after being incorporated into DNA leads to cell death (cf. Hamada et al. (2002) for the metabolic pathway). This incorporation into DNA can only take place during the proliferation phase while cells without active DNA replication remain unaffected. AraC operates non-specifically, thus affecting the blasts as well as the HSCs. This can lead to severe hematopoiesis suppression, a real and serious side effect called Leukopenia. As a consequence, the immune system is not capable to adequately react which can result in life threatening infections. Leukopenia is characterized by absolute L counts below one thousand

⋆ This research was supported by a research grant of the "nternational Max Planck Research School (IMPRS) for Advanced Methods in Process and System Engineering (Magdeburg)" and from the European Research Council via the Consolidator Grant MODEST-647573.


10.1016/j.ifacol.2016.12.101

cells per microliter blood. The longer this state lasts the higher the mortality. The susceptibility to leukopenia due to chemotherapy shows a large variability among patients.

Mathematical modeling can form a basis for advanced patient-specific analysis and decision support tools. Such a mathematical model must be able to reproduce and in a later stage also predict qualitatively and quantitatively patterns of L during chemotherapy treatment. This retrospective study with the presented mathematical model is a promising start towards advanced patient-specific leukopenia treatment and decision support tools.

## 2. MATERIALS AND METHODS

### *2.1 Clinical data*

Measurement data of L and therapy plans for six AML patients (denoted by P1, . . . , P6) are provided by the Department of Hematology and Oncology of the University Hospital in Magdeburg (Figure 1 and Table 1).

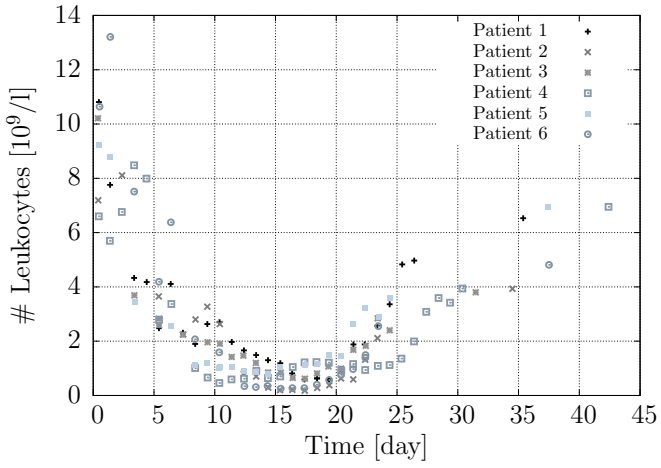


Fig. 1. Measurement data of the six patients, periods ranging from 32 to 43 days.

Here, the first consolidation cycle is considered in which AML was prevented by administer AraC. One consolidation cycle consists of two AraC infusions at day one, three and five. The two infusions last three hours each with a 12 hours in between. The values for the body surface are calculated using DuBois formula (cf. DuBois et al. (2013)).

Table 1. Patient-specific physiological properties, cytarabine application per infusion and numbers of measurements.

| | Sex | Age | Height | Weight | BSA∗ | Cyt. per inf. | Meas. |
|---|---|---|---|---|---|---|---|
| | - | (year) | (cm) | (kg) | ($m^2$) | (mg/$m^2$) | (#) |
| P1 | F | 61 | 175 | 92 | 1.92 | 3000 | 29 |
| P2 | M | 67 | 176 | 74 | 1.89 | 1000 | 20 |
| P3 | F | 74 | 170 | 81 | 1.81 | 1000 | 23 |
| P4 | F | 49 | 170 | 71 | 1.83 | 3000 | 31 |
| P5 | F | 30 | 166 | 75 | 1.72 | 3000 | 22 |
| P6 | M | 64 | 190 | 80 | 2.00 | 3000 | 21 |

∗ BSA = body surface area

### *2.2 Mathematical model*

Since we are focusing on leukopenia during consolidation therapy, we exclusively simulate the dynamics of the

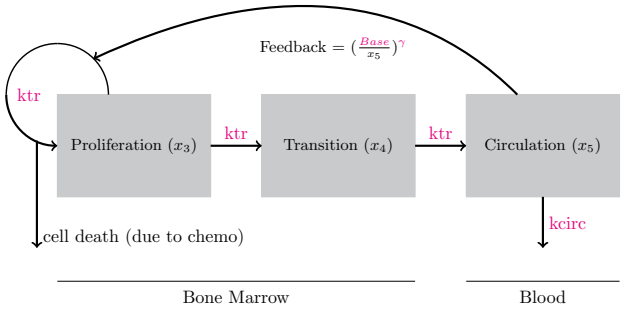


Fig. 2. Schematic model of leukocyte cells' dynamics

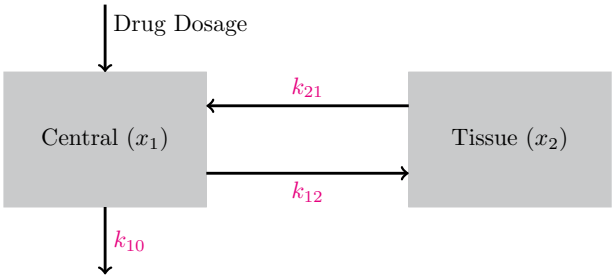


Fig. 3. Two-compartment model describing the pharmacokinetics of the drug cytarabine.

healthy immune cells (L) within the blood stream. The drug impact is accounted for by additional states for pharmacokinetics (PK) and a pharmacodynamic (PD) function.

In order to describe the cell dynamics, we use a compartment model based on Friberg et al. (2002). Referring to the cell differentiation process, the cell-line consists of (i) a proliferating compartment PC sensitive to chemotherapy, (ii) transit compartments TC representing diverse differentiation states and (iii) a compartment with mature, circulating blood cells MC. Savic et al. (2007) showed that the number of transition compartments models the delay between the proliferating cells and circulating cells. As the intermediate maturation steps are of no interest in our setting, and the numerical results indicate that the delay is well captured by using one compartment, we simplified Friberg's model by using one instead of three transition compartments (Figure 2).

Cells mature with a transition rate $ktr$ from the precursor compartment. MCs ($x_5$) are removed from the blood stream with a death rate of $kcirc$. In order to respond to cell decline, matured cells influence the proliferation rate of proliferating cells by a feedback loop.

A two-compartment model is used for PK (Figure 3). The PD is modeled by a log-linear function $E$.

The five differential states of our mathematical model are the amounts $x_1, x_2$ of AraC in two compartments, and the numbers $x_3, x_4, x_5$ of L in three compartments. The external input is the dose of AraC $u(t)$. The mathematical model is defined by the following equations:

**Pharmacokinetics:** (1)

$$\dot{x}_1(t) = -k_{10} \cdot x_1(t) - k_{12} \cdot x_1(t) + k_{21} \cdot x_2(t) + \frac{u(t) \cdot \text{BSA}}{\text{duration}}, \quad (2)$$

$$\dot{x}_2(t) = k_{12} \cdot x_1(t) - k_{21} \cdot x_2(t), \quad (3)$$

**Pharmacodynamics:**

$$E = slope \cdot ln\left(1.0 + \frac{x_1(t)}{V \cdot MM_{cyt}}\right), \quad (4)$$

**Leukopenia Model:**

$$\dot{x}_3(t) = ktr \cdot x_3(t) \cdot \left(\left(\frac{Base}{x_5(t)}\right)^{\gamma} - 1\right) - E \cdot x_3(t), \quad (5)$$

$$\dot{x}_4(t) = ktr \cdot (x_3(t) - x_4(t)), \quad (6)$$

$$\dot{x}_5(t) = ktr \cdot x_4(t) - kcirc \cdot x_5(t), \quad (7)$$

**Initial Values:**

$$x_1(0) = 0.0, \quad (8)$$

$$x_2(0) = 0.0, \quad (9)$$

$$x_3(0) = \frac{Base \cdot kcirc}{ktr}, \quad (10)$$

$$x_4(0) = \frac{Base \cdot kcirc}{ktr}, \quad (11)$$

$$x_5(0) = Base_0. \quad (12)$$

Note that we used two approaches to cope with the initial values: (i) to use (1-12) with two different parameters $Base$ and $Base_0$, as in Nock (2013) and (ii) to enforce equality between the two via

$$Base = Base_0 \quad (13)$$

as suggested by Quartino et al. (2012) (leading to equilibrium. We will refer to (1-13) as I1 and to (1-12) as I2.

A summary of model parameters, constants and the control within (1-12) are listed in Table 2. Furthermore, the system is summarized as $\dot{x}(t) = f(x(t), p)$, where the external stimulus and some fixed constants become part of the function $f(\cdot)$.

Table 2. Model parameters (p) and control u(t) with units

| $p$ | ktr | kcirc | $\gamma$ | Base / Base0 | slope | $u(t)$ |
|---|---|---|---|---|---|---|
| Unit | $1/day$ | $1/day$ | - | $\# \cdot 10^9/l$ | $l/mol$ | $mg/m^2$ |

### *2.3 Parameter estimation*

Let a set of one-dimensional measurements $\eta_1, \ldots, \eta_m$ and known variances $\sigma_i^2$ at time points $t_1, \ldots, t_m$ be given. Assume that the measurements can be described by a nonlinear regression

$$\eta_i = h(x^*(t_i), p^*) + \varepsilon_i \quad (14)$$

with the model response function $h$ of the true but unknown states $x^*$ and parameters $p^*$ and the independent and identically distributed measurement errors $\varepsilon_i \sim \mathcal{N}(0, \sigma_i)$.

Solving the nonlinear weighted least squares problem

$$\min_p \quad \frac{1}{2}\sum_i^m \frac{(\eta_i - h(x(t_i), p))^2}{\sigma_i^2} \quad (15a)$$

$$\text{s.t.} \quad \dot{x}(t) = f(x(t), p) \quad (15b)$$

$$x(t_0) = x_0, \quad (15c)$$

with different approaches to determine the variances

$$\sigma_i = \begin{cases} 1, & \text{(W1)} \\ \eta_i, & \text{(W2)} \\ if\ (\eta_i \geq 1) : \sqrt{\eta_i},\ else:\ {\eta_i}^2. & \text{(W3)} \end{cases}$$

yields parameters $\hat{p}$ which fit the model response to the data. The dynamic process described by a system of ordinary differential equations is formulated as an implicit constraint.

The parameter estimations are performed with three different weighting techniques W1–W3 for $\sigma_i$ (as suggested above). W1 is an unweighted least square, a standard method in parameter estimation. Thereby, measurements close to zero are less influential on the objective. Since our focus is on leukopenia (i.e. values below one), we introduced two more weighting methods W2 and W3. W2 can be seen as a scaling method, whereby the squared deviations are scaled by the original values of $\eta_i$ leading to higher weighting of low $\eta_i$. To make values between one and zero more influential on the objective but without loosing too much informations of higher values of L, we differentiate weigthings of measurements below and above one (W3). Please notice, the value of one refers to our unit of L, i.e. $10^9$ cells per $\mu l$.

As the measurement error $\varepsilon$ is a random variable, also the solution $\hat{p}$ is a random variable which is in first order normally distributed with mean $p^*$ (true but unknown value) and variance-covariance matrix $C = (J^T J)^{-1}$ with $J$ as the derivative of the objective of (15) with respect to $p$. The confidence regions of the parameters in which the true parameter values are located to a certain probability $1 - \alpha$ are nonlinear and thus difficult to compute. So, linearized confidence regions are computed

$$CR(\hat{p}, \alpha) = \{p : (p - \hat{p})^T C (p - \hat{p}) \leq \chi^2_{n_p}(1 - \alpha)\} \quad (16)$$

with $\chi^2_{n_p}$ as the $\chi^2$ distribution with $n_p$ degrees of freedom. We obtain estimates for standard deviations from entries on the main diagonal of $C$.

Theoretically, all unknowns in (1-13) can be used in a parameter estimation. However, based on measurements of MCs alone, certain parameters can not be identified. Therefore we fix some of them to constant values. This concerns the parameters (constants) $k_{10}$, $k_{12}$, $k_{21}$ and $V$ from PK. We used published data from Kern et al. (1997) in order to estimate these PK parameters by ordinary least squares (Table 3).

Table 3. Values of the constant parameters of the PK model ($k_{10}, k_{12}, k_{21}$ and Volume (V)), molar mass of cytarabine (MM) and duration of cytarabine infusion (d).

| Constants | $k_{10}$ | $k_{12}$ | $k_{21}$ | V | MM | d |
|---|---|---|---|---|---|---|
| Value | 98.64 | 2.69 | 1.29 | 37.33 | 243.217 | 3/24 |
| Unit | 1/day | 1/day | 1/day | liter | g/mol | day |

We gratefully acknowledge the use of the parameter estimation software tool PAREMERA from Körkel and colleagues, c.f. Kircheis (2015). It is implemented in VPLAN (c.f. Körkel (2002)) and is based on a Gauß-Newton approach. VPLAN provides an all-at-once solution to solve parameter estimation problems with Internal Numerical

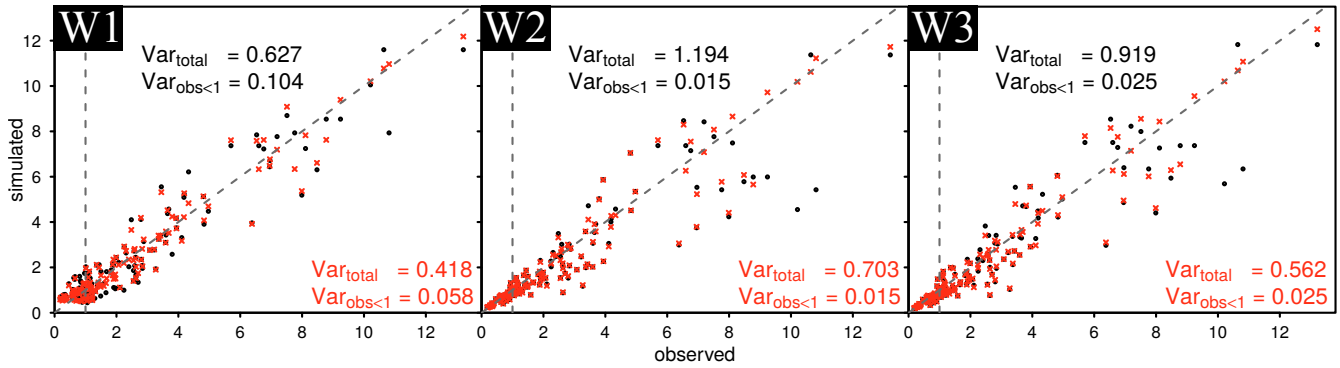


Fig. 4. Calculation of the error variances between model response after parameter estimation and observations. Initial approach I1 in black, I2 in red. $\mathrm{Var}_{total}$ = error variances calculated with all measurments, $\mathrm{Var}_{obs<1}$ = error variances calculated with measurements below 1.

Differentiation, c.f. Bock (1987) and automatic differentiation of model functions via ADIFOR, c.f. Bischof et al. (1996).

## 3. NUMERICAL RESULTS

We started our analysis by treating all six AML patients as a population (P0) resulting in 146 measurements. Therewith sets of parameter values are computed for the two different initial value approaches I1, I2 and the different weighting techniques W1–W3. Afterward, these population-based parameters were used as initial values (Table 4) for estimating an individual set of parameters for each patient (P1–P6).

Table 4. Initial parameter values (M) with their absolute standard deviations (SD) for the two initial value approaches I1 and I2.

| | Base | | gamma | | ktr | | slope | | Base0 | |
|---|---|---|---|---|---|---|---|---|---|---|
| INIT | M | SD | M | SD | M | SD | M | SD | M | SD |
| I1 | 10.00 | 0.27 | 0.18 | 0.02 | 0.50 | 0.04 | 0.91 | 0.06 | - | - |
| I2 | 10.00 | 0.37 | 0.18 | 0.02 | 0.50 | 0.05 | 0.91 | 0.05 | 10.00 | 1.17 |

A comparison of simulated vs. observed values illustrated the major differences between the different weighting techniques (Figure 4). The two alternative weighting techniques W2 and W3 showed an improved fit at low values of observed L concentrations (e.g. below 1). This was also illustrated by calculating the error variances (i.e. the variance VAR of the paired differences between simulated and observed values) for the different trajectories. While W1 necessarily showed the lowest overall error variances, W2 and W3 appeared to have much lower error variances at low L concentrations ($L_{obs} < 1$). In summary, W1 is the best overall fit, whereas W2 is the best fit for L below one (Figure 4). From a practical point of view, however, W3 is a very powerful compromise combining the advantages of both with a still good overall fit (better than W2) and a comparatively good fit for L below one (better than W1). This pattern was even independent of the used initial value approach. Furthermore, we calculated the unweighted sum of squares for the I1–I2 and W1–W3 (see Table 5) for assessing overall model performance. As mentioned above, W3 appeared to be superior to W2 and is a good choice for estimating parameters in leucopenia models. Therefore, we are focusing the following analysis on W3 as it constitutes the most promising weighting technique in our setting.

I2 shows for all three weighting methods lower error variances comparing to I1 (Figure 4). This is a matter of fact given the addition degree of freedom provided by the addition parameter $Base_0$ in I2.

Table 5. Squared values for the six individual patients P1–P6 for I1–I2 and W1- W3.

| | | P1 | P2 | P3 | P4 | P5 | P6 |
|---|---|---|---|---|---|---|---|
| I1 | W1 | 25.10 | 8.27 | 11.43 | 7.58 | 24.28 | 14.39 |
| | W2 | 43.41 | 23.61 | 35.07 | 15.87 | 46.54 | 22.54 |
| | W3 | 32.98 | 11.43 | 25.11 | 16.59 | 35.24 | 19.90 |
| I2 | W1 | 9.33 | 6.63 | 1.76 | 6.83 | 22.84 | 13.18 |
| | W2 | 12.48 | 14.90 | 2.75 | 13.94 | 44.18 | 20.67 |
| | W3 | 11.28 | 8.74 | 2.44 | 14.38 | 20.67 | 17.11 |

Table 6 shows the resulting estimated parameter values with their absolute standard deviations. One observes significant differences between the individuals P1–P6. Also the values of the population fit P0 differ significantly, and lead to different dynamics as shown in Figures 5 and 6. The difference between individual and population fits illustrates the potential error that may arise from ignoring individual properties.

Table 6. Parameter values (M) with their absolute standard deviations (SD) for the population estimate P0 and the six individual estimates P1–P6, for both initial approaches I1–I2 and the weighting method W3.

| | Base | | gamma | | ktr | | slope | | Base0 | |
|---|---|---|---|---|---|---|---|---|---|---|
| I1 | M | SD | M | SD | M | SD | M | SD | M | SD |
| P0 | 6.90 | 0.27 | 0.40 | 0.03 | 0.26 | 0.02 | 3.09 | 0.45 | - | - |
| P1 | 6.34 | 0.58 | 0.71 | 0.15 | 0.16 | 0.03 | 1.59 | 0.34 | - | - |
| P2 | 8.23 | 0.77 | 0.26 | 0.07 | 0.29 | 0.05 | 2.63 | 0.82 | - | - |
| P3 | 5.69 | 0.77 | 0.44 | 0.18 | 0.20 | 0.05 | 1.55 | 0.42 | - | - |
| P4 | 7.51 | 0.55 | 0.12 | 0.05 | 0.46 | 0.12 | 0.89 | 0.19 | - | - |
| P5 | 7.37 | 0.65 | 0.24 | 0.09 | 0.33 | 0.08 | 0.93 | 0.22 | - | - |
| P6 | 11.83 | 0.67 | 0.16 | 0.04 | 0.36 | 0.05 | 1.39 | 0.30 | - | - |
| I2 | M | SD | M | SD | M | SD | M | SD | M | SD |
| P0 | 6.64 | 0.36 | 0.36 | 0.04 | 0.26 | 0.02 | 2.03 | 0.27 | 13.0 | 1.42 |
| P1 | 5.40 | 0.74 | 0.87 | 0.26 | 0.14 | 0.03 | 1.64 | 0.37 | 22.8 | 3.50 |
| P2 | 9.66 | 1.23 | 0.23 | 0.06 | 0.31 | 0.06 | 1.95 | 0.59 | 2.96 | 3.32 |
| P3 | 4.16 | 1.06 | 0.76 | 0.48 | 0.15 | 0.06 | 1.59 | 0.52 | 19.5 | 3.00 |
| P4 | 7.95 | 0.67 | 0.11 | 0.04 | 0.47 | 0.12 | 0.90 | 0.19 | 2.30 | 3.26 |
| P5 | 6.18 | 0.87 | 0.34 | 0.16 | 0.27 | 0.08 | 0.94 | 0.27 | 17.3 | 3.98 |
| P6 | 12.71 | 0.98 | 0.15 | 0.04 | 0.37 | 0.06 | 1.40 | 0.30 | 5.64 | 4.42 |

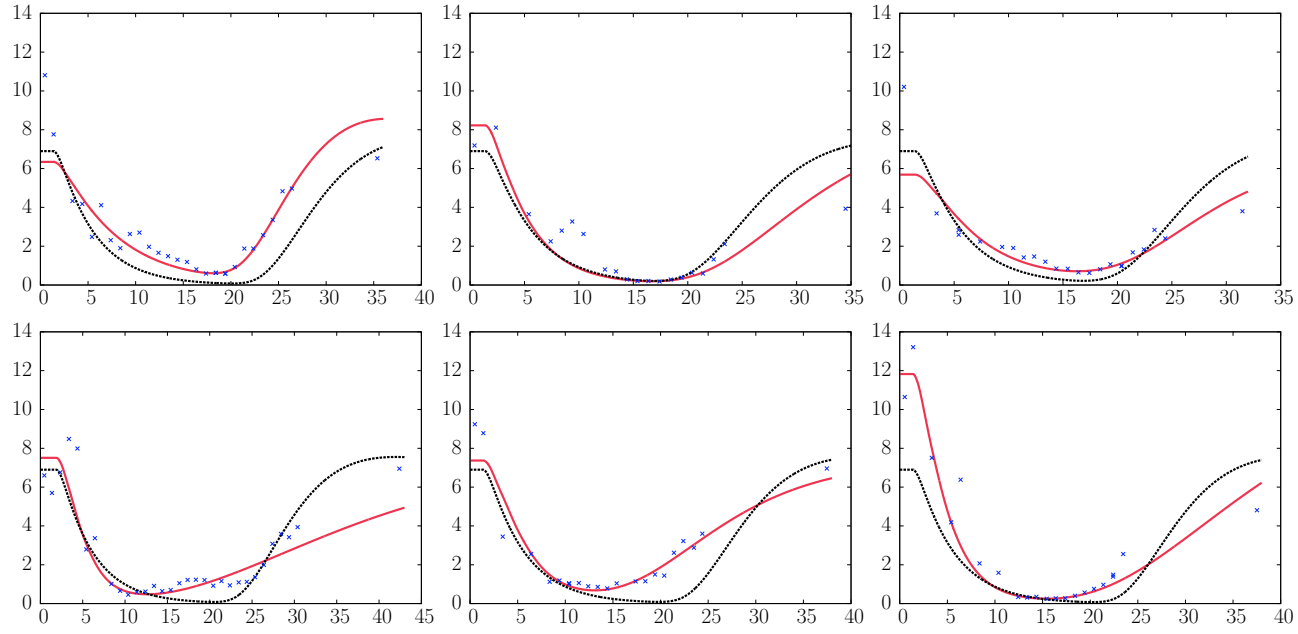

Fig. 5. Dynamics of circulating leukocytes $x_5$ (y axis: # of leukocytes $[10^9/l]$) over time (x axis: time [day]) with initial value approach I1 and our weighting technique W3 (——) for all six patients P1–P6. As a reference the trajectories for the population fit P0 (·····) with I1 and W3 are shown.

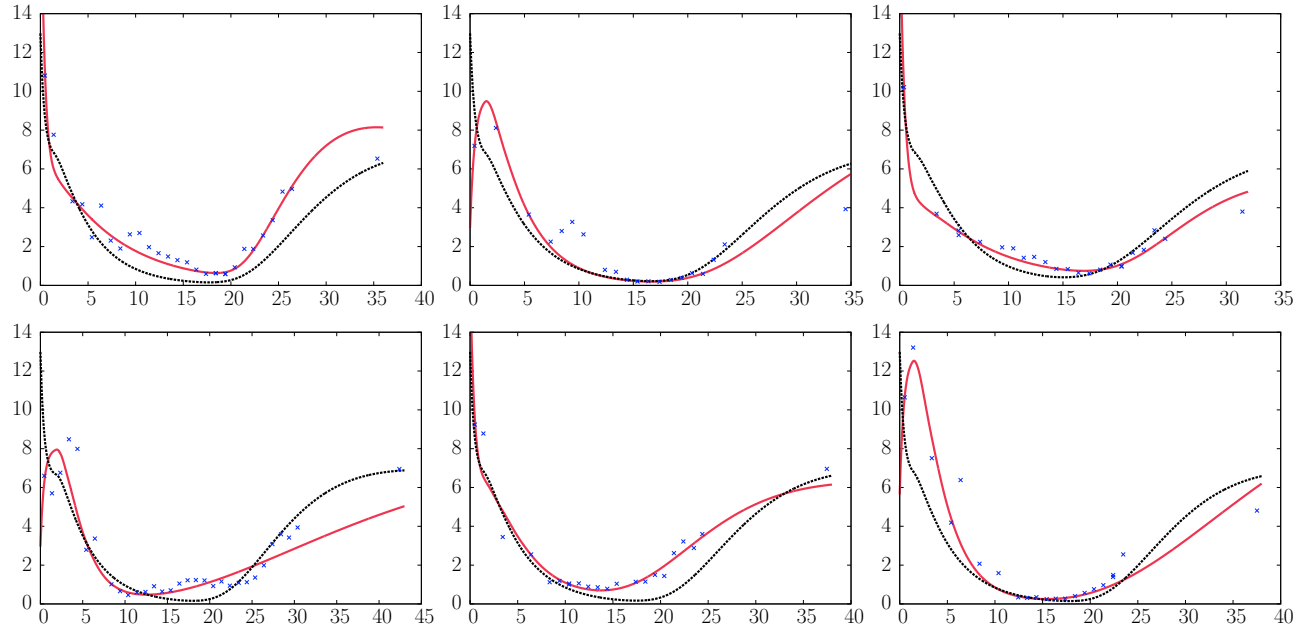

Fig. 6. As Figure 5, but with initial value approach I2. Note how the additional degree of freedom $Base_0$ for the initial value $x_5(0)$ is used to obtain overall better fits compared to Figure 5.

## 4. DISCUSSION AND CONCLUSION

Our results show differences in the patient-specific parameters and therewith in the quality of L dynamics compared to P0 as well as compared to each other. Generally, patients respond differently to the same amount of an administered drug. Therefore, patient-specific diagnosis and therapy are becoming more and more established. In order to account for such an individualized treatment, knowledge about individual physiological characteristics is essential. *In vivo* measurements of patients-specific agent concentrations in relevant compartments (e.g., blood plasma) will help to generate individual PK profiles and therewith provide tools for the prediction of agent concentration dynamics at the side of action. *In vitro* measurements of agent toxicity, can similarly be used for developing corresponding (PD) profiles (e.g. Bennett et al. (2014)) and therewith provide cytotoxic profiles for the applied agent. A combination of *in vivo* and *in vitro* measurements linked with *in silico* modeling will provide a powerful methodology (Fuentes et al. (2009)) to generate the required information about individualized physiological properties and the corresponding treatment adaptations, requirements, and risks. Moreover, models can help to identify optimized

sampling protocols for clinical practise, e.g. as proposed by Jost et al. (2016). Such modeling tools are required for projections of therapy success, recovery progress as well as the corresponding personalized optimization of therapy schedules. We therefore conclude that patient-specific measurements and parameter estimations are definitely necessary to come up with optimized individual treatments. A larger cohort of patients would improve our ability to estimate parameter variation among individuals and will enable statistical analysis (e.g. parameter depending sensitivity against leukopenia) as well as the opportunity to predict patient-specific reactions on chemotherapy treatment.

Concerning the different approaches to incorporate initial values I1 and I2, there is no clear winner. Whereas the additional degree of freedom $Base_0$ in approach I2 is used to fit the steep decline of L better (and also a short increase which is plausible because of delays of the chemotherapy), approach I1 guarantees the start from a steady state, which seems biologically more plausible. However, the initial values have a deep impact on parameter values (e.g. $Base0$ correlates with $ktr, \gamma$ and $Base$). Therefore, more detailed studies on this and a larger cohort of patients are required.

With respect to the three different weighting strategies W1–W3, we prefer W3, as it highlights the crucial and relevant time horizon when the number of L is down and a leukopenia may occur but also take higher values of L into account, when recovering from leukopenia. The resulting, more conservative underestimation $x_5(t)$ has an intrinsic safeguard against model uncertainty.

In summary, the resulting simulations give a good fit to the measurements and would be an adequate basis for clinical decision support. Future work needs to evaluate the prospective prediction accuracy, based on parameter estimates from previous treatment cycles and applied in a real-time context.

## REFERENCES


Bennett, T.A., Montesinos, P., Moscardo, F., Martinez-Cuadron, D., Martinez, J., Sierra, J., García, R., de Oteyza, J.P., Fernandez, P., Serrano, J., et al. (2014). Pharmacological profiles of acute myeloid leukemia treatments in patient samples by automated flow cytometry: a bridge to individualized medicine. *Clin Lymphoma Myeloma Leuk*, 14(4), 305–318.

Bischof, C., Carle, A., Khademi, P., and Mauer, A. (1996). ADIFOR 2.0: Automatic Differentiation of Fortran 77 Programs. *IEEE Comput Sci Eng*, 3, 18–32.

Bock, H. (1987). *Randwertproblemmethoden zur Parameteridentifizierung in Systemen nichtlinearer Differentialgleichungen*, volume 183 of *Bonner Math Schriften*. Universität Bonn, Bonn. URL `http://www.iwr.uni-heidelberg.de/groups/agbock/FILES/Bock1987.pdf`.

DuBois, C., Farnham, J., Aaaron, E., and Radunskaya, A. (2013). A multiple time-scale computational model of a tumor and its micro environment. *Math Biosci Eng*, 10(1), 121 – 150.

Eigendorff, E. and Hochhaus, A. (2015). Akute leukämien des erwachsenen. *Pathologe*, 36(5), 503–519.

Friberg, L., Henningsson, A., Maas, H., Nguyen, L., and Karlsson, M. (2002). Model of Chemotherapy-Induced Myelosuppression with Parameter Consistency Across Drugs. *J Clin Oncol*, 20, 4713–4721.

Fuentes, D., Oden, J.T., Diller, K.R., Hazle, J.D., Elliott, A., Shetty, A., and Stafford, R.J. (2009). Computational modeling and real-time control of patient-specific laser treatment of cancer. *Ann Biomed Eng*, 37(4), 763–782. doi:10.1007/s10439-008-9631-8.

Hamada, A., Kawaguchi, T., and Nakano, M. (2002). Clinical pharmacokinetics of cytarabine formulations. *Clin Pharmacokinet*, 41(10), 705–718. doi:10.2165/00003088-200241100-00002.

Jost, F., Rinke, K., Fischer, T., Schalk, E., and Sager, S. (2016). Optimum experimental design for patient specific mathematical leukopenia models. In *Proc. of the Foundations of Systems Biology in Engineering (FOSBE) Conference*. Magdeburg, Germany.

Kern, W., Schleyer, E., Unterhalt, M., Wörmann, B., Büchner, T., and Hiddemann, W. (1997). High antileukemic activity of sequential high dose cytosine arabinoside and mitoxantrone in patients with refractory acute leukemias. *Cancer*, 79(1), 59–68.

Kircheis, R. (2015). *Structure exploiting parameter estimation and optimum experimental design methods and applications in microbial enhanced oil recovery.* Heidelberg: Univ. Heidelberg, Naturwissenschaftlich-Mathematische Gesamtfakultät (Diss.).

Körkel, S. (2002). *Numerische Methoden für Optimale Versuchsplanungsprobleme bei nichtlinearen DAE-Modellen*. Ph.D. thesis, Universität Heidelberg, Heidelberg. URL `http://www.koerkel.de`.

Nock, V. (2013). *Pharmacometric modelling of processes in the haematopoietic system and blood*. Ph.D. thesis, Freie Universität Berlin.

Quartino, A., Friberg, L., and Karlsson, M. (2012). A simultaneous analysis of the time-course of leukocytes and neutrophils following docetaxel administration using a semi-mechanistic myelosuppression model. *Invest new Drug*, 30, 833–845.

Savic, R.M., Jonker, D.M., Kerbusch, T., and Karlsson, M.O. (2007). Implementation of a transit compartment model for describing drug absorption in pharmacokinetic studies. *J Pharmacokinet Pharmacodyn*, 34(5), 711–726.